Simulation of liquid composite molding processes using a generic mixed FE-SPH method

Sébastien Comas-Cardona* — Paul H.L. Groenenboom**
Christophe Binétruy* — Patricia Krawczak*

** Ecole des Mines de Douai, Technology of Polymers and Composites Department*
941 rue Bourseul, BP 838, F-59508 Douai cedex

binetruy@ensm-douai.fr

*** Engineering Systems International-BV, Gebouw Kortland,*
Nieuwe Tiendweg 11a, 2922 EN Krimpen aan den IJssel, The Netherlands

pg@esibv.nl

ABSTRACT. *Composite manufacturing processes involve multi-scale phenomena. Equations governing mechanics, heat transfer and fluid flow dynamics can be derived in the scale of the problem to solve. This article focuses on addressing fluid flow simulation needs for Liquid Composite Molding processes using a generic mixed FE-SPH method. The SPH method is Lagrangian and models fluids as particles. The method has been proven to be suitable to simulate fluid flows. Special solutions have been developed for flow through porous media and non-Newtonian fluid flow. Numerical schemes for such solutions are also given. The implementation of the SPH algorithm within a structural finite element software facilitates simulation of fluid-structure for LCM processes. Several applications are presented and discussed.*

RÉSUMÉ. *La fabrication de matériaux composites met en jeu des phénomènes multiéchelles. Les équations qui gouvernent la dynamique des fluides, la mécanique et le transfert thermique peuvent être développées à l'échelle du phénomène à observer. Cet article se focalise sur les besoins de simulation des moulages composites en utilisant une méthode générique FE-SPH. La méthode SPH est lagrangienne et modélise le fluide à l'aide de particules. Il a été prouvé que cette méthode est appropriée pour simuler et modéliser l'écoulement de fluides. Des solutions spéciales ont été développées pour l'écoulement dans un milieu poreux et pour un fluide non newtonien. Les schémas d'intégration numérique sont également présentés. Les particules représentant le fluide peuvent interagir avec des éléments finis, ce qui permet de simuler des procédés de fabrication requérant des physiques couplées. Plusieurs applications sont présentées et discutées.*

KEYWORDS: *Smoothed Particle Hydrodynamics, finite elements, liquid composite molding, explicit numerical schemes.*

MOTS-CLES : Smoothed Particle Hydrodynamics, *éléments finis,* liquid composite molding, *schémas d'intégration explicite.*

REEF – 14/2005. Composites forming simulation, pages 867 to 883

1. Introduction

Composite materials are covering a wide range of applications for aeronautics, automotive and marine structures. Such composite materials are usually made of fibers enclosed in a thermosetting or thermoplastic matrix. Liquid Composite Molding (LCM) processes, such as compression, Resin Transfer Molding (RTM) or Vacuum Assisted Resin Transfer Molding (VARTM), have become of increasing interest to manufacture composite parts. Reproducibility, quality, performances, environment friendliness and cost reduction are goals a composite manufacturing company seeks. Those goals will inevitably require the use of reliable and powerful simulation tools that enhances predictions and reduces trial and error procedures.

It is well established that micro-, meso- and macroscale media are present in composite manufacturing processes. For instance, for continuous fiber reinforced composites, the microscale corresponds to the inner tow region, whereas the inter tow region would be mesoscale, and the macroscale represents the overall composite structure. Equations governing mechanics, heat transfer or fluid flow can be derived for the three scales depending on the problem to be solved or the phenomenon looked at. More precisely for fluid flow simulation, the Navier-Stokes equations, averaged Navier-Stokes for porous media (Tucker *et al*., 1994), or Darcy's law will be generally used. The equations are usually discretized in an Eulerian reference frame using Finite Difference Method (FDM) or Finite Element Method (FEM) (Trochu *et al*., 1993). However, when the geometry of the flow domain changes, because of interfaces with moving structures (such as compression, injection-compression or VARTM) or the presence of a free surface, special solutions are required. Also when coupling is present, *e.g.* hydro-mechanical coupling, (Han *et al.*, 1993) showed that mixed Control Volume/FDM can be used. (Also Kang *et al*., 2001 and Acheson *et al*., 2004) coupled resin flow, fiber preform mechanics and tow saturation during VARTM process through Control Volume/FEM or FDM algorithms. Those Eulerian numerical schemes are limited to small deformations for instance or do not allow to mix domains with porous and non-porous media. Lately, Lagrangian numerical schemes have been of interest with (Farina *et al.* 1997; Belov *et al*., 2004 and Sawley *et al*., 1999). The later qualitatively reproduced the flow front shape of an isothermal RTM filling using the Smoothed Particle Hydrodynamics (SPH) method for mesoscale simulations.

This paper particularly focuses on the use of the generic mixed FE-SPH method to address the simulation needs of LCM processes. First, fundamentals on fluid flow dynamics are given for porous and non-porous regions. Then, a detailed description of the mixed FE-SPH method is presented. Finally, several examples of applications for LCM simulations will be proposed and discussed.

2. Fluid flow dynamics

In the following sections, a bold lower case letter represents a vector and a bold upper case letter denotes a tensor.

2.1. *Fluid flow through porous media*

(Tucker *et al*., 1994) and Pillai 2002) derived the conservation of mass and momentum equations for flow in porous media from averaging the conservation equations for a two-phase medium in which one of the materials is fixed in space. In that case, the volume fraction available for the fluid remains fixed and is also called porosity. Considering laminar flow, the suitable forms of the equations to be solved (conservation of mass and momentum) are respectively:

$$\frac{\partial \eta}{\partial t} + \nabla \cdot (\eta \mathbf{u}) = 0 \qquad [1]$$

$$\frac{\partial \eta \mathbf{u}}{\partial t} + \nabla \cdot \eta \mathbf{u}\mathbf{u} = -\phi \nabla p + \phi \nabla(\boldsymbol{\tau}) + \eta \mathbf{g} - \phi^2 \mu \mathbf{K}^{-1} \cdot \mathbf{u} \qquad [2]$$

where ϕ is the fluid volume fraction or porosity, $\mathbf{u}$ the fluid velocity, μ the viscosity, $\boldsymbol{\tau}$ the viscous stress tensor, p the pressure, $\mathbf{g}$ the gravitational acceleration, $\mathbf{K}$ the permeability (tensor or scalar) and $\eta = \rho \phi$ the apparent density where ρ is the fluid density. For Equation 2, it has been assumed that the flow velocity in the porous region is small enough to assume that the viscous drag depends linearly on the velocity.

A scaling analysis can show that the viscous term (*i.e*., the second term of the RHS) can be, in most cases, neglected for LCM. With this assumption and using Equation 1, Equation 2 becomes:

$$\eta \left\{ \frac{\partial \mathbf{u}}{\partial t} + \mathbf{u}(\nabla \cdot \mathbf{u}) \right\} = -\phi \nabla p + \eta \mathbf{g} - \phi^2 \mu \mathbf{K}^{-1} \cdot \mathbf{u} \qquad [3]$$

Most of the time, the computational domain can be divided in porous (*e.g*., fiber reinforcements) and non-porous (*e.g*., channels or tubing) regions. In order to simulate the flow for all regions, Equation 3 provides the basis of the solution with the viscous drag term only being used within the porous domains. As a limiting case, within the porous region (*i.e*., where the flow is dominated by the viscous drag) the convective and inertia terms (LHS of Equation 3) becomes negligible and therefore Darcy's law for the transport (or filtration) velocity $\mathbf{v} = \phi \mathbf{u}$ may be verified.

2.2. *Non-Newtonian fluid flow*

For the flow of a liquid around individual and immersed solid objects, the following conservation of mass and Navier-Stokes equations should be solved:

$$\frac{\partial \rho}{\partial t} + \nabla \cdot (\rho \mathbf{u}) = 0 \qquad [4]$$

$$\rho \left\{ \frac{\partial \mathbf{u}}{\partial t} + \mathbf{u}(\nabla \cdot \mathbf{u}) \right\} = -\nabla p + \nabla(\boldsymbol{\tau}) + \mathbf{g} \qquad [5]$$

For composite molding conditions, turbulence is irrelevant, but non-Newtonian laminar flow should be considered. The components of the viscous stress tensor may be written as:

$$\tau_{ij} = \mu \left(\frac{\partial u_i}{\partial x_j} + \frac{\partial u_j}{\partial x_i} \right) - \frac{2\mu}{3} \frac{\partial u_k}{\partial x_k} \delta_{ij} \qquad [6]$$

where the indices *i, j,* and *k* refer to the three Cartesian coordinates and δ_{ij} is the Kronecker delta. Note that the divergence term on the RHS of Equation 6 is maintained since limited compressibility will be assumed in the SPH formulation (Equation 15), but maintain as low as possible (see Sections 2.3 and 3.3). Among several non-Newtonian rheological models, the Carreau one will be chosen because it can model fairly well most polymeric fluid behaviors (McCabe *et al.*, 2002; Achilleos *et al.*, 2002):

$$\mu = \mu_\infty + (\mu_0 - \mu_\infty) \left[1 + (\xi E)^\alpha \right]^{\frac{\beta - 1}{\alpha}} \qquad [7]$$

where E is the total strain rate and α, β, ξ, μ_0 and μ_∞ are all parameters of the fluid to be fitted to experimental data. The asymptotic behavior at large E is Newtonian with a viscosity of μ_∞, for small E the effective viscosity tends to μ_0, and at intermediate regime it displays shear-thinning behavior rather like a power-law fluid. Since this model does not contain a yield stress, nor infinities at any limit, no numerical instabilities are expected. Note that if $\mu_0 = \mu_\infty$ Equation 7 models a Newtonian fluid.

2.3. *Compressible fluid formulation*

During composite molding, the flow of resin may be considered as incompressible. In that case Equation 1 and 4 would reduce to $\nabla.\mathbf{u} = 0$ and the pressure should be obtained from a Poisson type of equation. Such a system of

equations can be solved efficiently by an implicit method which allows for a relatively large time step. In the present study, however, the solution time step needs to be small. The first reason is that the motion of the flow front requires an accurate solution in time and space when the resin passes the border of the porous region. A second reason is that the weak coupling of the flow with moving structures for instance, requires an explicit solution with a sufficiently small time step. If the time step has to be small, an explicit solution in combination with compressibility of the liquid is more suitable.

3. Smoothed particle hydrodynamics fundamentals

The fully Lagrangian and meshless SPH method has been originally developed by (Gingold *et al.*, 1977) and Lucy 1977) to solve astrophysical problems. Later, (Monaghan 1983, 1994) applied the SPH method to the flow of compressible fluids and also showed that when pressure wave propagation is not of prime interest (as in LCM simulations), the use of an artificial equation of state is quite suitable to model incompressible fluid flows. SPH solutions for incompressible flow have also been developed, but such solutions have not been pursued for LCM simulations.

3.1. *Integral interpolants and kernel functions*

Mathematically, an integral interpolant of an arbitrary function $\varphi(\mathbf{r})$ can be defined as:

$$\langle \varphi(\mathbf{r}) \rangle = \int_{\Omega} \varphi(\mathbf{r}') W(|\mathbf{r} - \mathbf{r}'|, h) \mathrm{d}\mathbf{r}' \quad [8]$$

where W is a kernel function having the following properties:

$$\begin{cases} \int_{\Omega} W(\mathbf{r}, h) \mathrm{d}\mathbf{r} = 1 \\ W(\mathbf{r}, h) \to \delta(\mathbf{r}) \text{ when } |\mathbf{r}| \to 0 \\ W(\mathbf{r}, h) = 0 \text{ when } \mathbf{r} \geq \lambda h \end{cases} \quad [9]$$

where $\mathbf{r}$ is the vector position, h a scalar called the smoothing length, λ a constant parameter taken as 2, δ the Dirac function and Ω the domain. The integral interpolant is an estimate of the function φ. Moreover, it can be shown that the integral interpolant of the gradient of a function, if the boundary integrals are neglected, may be written as:

$$\langle \nabla \varphi \rangle = \int_{\Omega} \varphi(\mathbf{r}') \nabla W(|\mathbf{r} - \mathbf{r}'|, h) \mathrm{d}\mathbf{r}' \quad [10]$$

From a choice of kernel functions available in the software, the frequently used cubic spline function has been chosen for this study. As quoted by Shao and Lo (2003), this kernel has compact support, a continuous second derivative and is not very sensitive to particle disorder.

3.2. *Summation interpolants*

For numerical simulation of continuum dynamics, the material is modeled by $a = 1, 2, \ldots N$ particles of mass m_a and density ρ_a. A particle a interacts with the neighboring particles b belonging to the sphere of influence of a. A sphere of influence (Figure 1), is defined by a kernel function that weighs interactions and a smoothing length that limits interactions in space. Therefore, the integral interpolant of a function (defined in section 3.1.) and its gradient can be approximated by a summation interpolant over a collection of particles:

$$\langle \varphi(\mathbf{r}_a) \rangle = \sum_b m_b \frac{\varphi_b}{\rho_b} W(|\mathbf{r}_a - \mathbf{r}_b|, h) \quad [11]$$

$$\langle \nabla \varphi(\mathbf{r}_a) \rangle = \sum_b m_b \frac{\varphi_b}{\rho_b} \nabla_a W(|\mathbf{r}_a - \mathbf{r}_b|, h) \quad [12]$$

Equation 12 shows that no mesh is required to numerically evaluate the gradient of the unknown functions but only the gradient of the kernel function. The role of grid or mesh size in FDM or FEM is played by the particle size in SPH: a smaller particle size implies a better spatial resolution of the flow, but requires more CPU. The smoothing length is defined to be proportional to the particle size.

The fact that SPH is a meshless method explains the attractiveness of the method to the dynamics of materials undergoing large relative displacements, while maintaining a Lagrangian frame of reference.

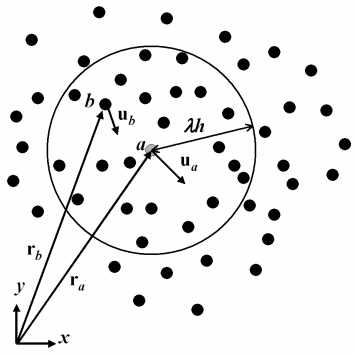

Figure 1. *Sphere of influence of a particle a*

3.3. *SPH formulation for fluid flow through porous media*

Within the SPH method, particles represent a fixed amount of material. If the fluid enters a porous region, the mass has to be distributed over a larger volume in space. Since the fluid particles should be able to model the progress of the flow front, the proper choice for the SPH formulation in porous media is to let the particles move with the microscopic fluid velocity. Thus, Equations 1 and 3 are amenable to the regular SPH discrete equations, which involves the apparent density and the microscopic velocity:

$$\frac{\mathrm{d}\eta_a}{\mathrm{d}t} = \sum_b m_b \left(\mathbf{u}_a - \mathbf{u}_b\right) \cdot \nabla_a W_{ab} \qquad [13]$$

$$\frac{\mathrm{d}\mathbf{u}_a}{\mathrm{d}t} = -\phi_a \sum_b m_b \left(\frac{p_b}{\eta_b^2} + \frac{p_a}{\eta_a^2} + \Pi_{ab} \right) \nabla_a W_{ab} + \mathbf{g} - \phi_a^2 \mu \mathbf{K}_a^{-1} \frac{\mathbf{u}_a}{\eta_a} \qquad [14]$$

The artificial viscosity contribution Π_{ab} from (Monaghan *et al.*, 1983) has been included in the momentum equation in order to stabilize the solution scheme. This type of artificial viscosity is superior to the standard finite element viscosity for SPH. For flow at low speed, the strength of the artificial viscosity may be taken quite small. For fluid flow through porous media, the most relevant physical viscosity contribution is directly entered as the viscous drag term of the momentum equation. Conservation of energy may also be solved with a similar SPH formulation, but since the pressure does not depend on the internal energy and since it will be assumed here that thermal effects on the viscosity may be neglected, the energy equation will not be considered.

Since Equations 13 and 14 allow some compressibility, they will be solved in combination with an artificial equation of state (Murnaghan model) for nearly incompressible liquid:

$$p = p_0 + B\left[\left(\frac{\rho}{\rho_0}\right)^{\gamma} - 1\right] \qquad [15]$$

with p_0 a reference pressure, ρ_0 the reference density, B the (artificial) bulk modulus and γ the exponent. The parameters B and γ are adjusted to keep the sound speed for Equation 15 greater, by at least a factor of 10, than the maximum fluid velocity. Therefore, tuning properly those parameters will keep the compressibility lower than a few percent.

3.4. *SPH formulation for non-Newtonian fluid flow*

A similar SPH formulation of Equations 4 and 5 can be given for non-Newtonian fluid flow:

$$\frac{\mathrm{d}\rho_a}{\mathrm{d}t} = \sum_b m_b \left(\mathbf{u}_a - \mathbf{u}_b\right) \cdot \nabla_a W_{ab} \qquad [16]$$

$$\frac{\mathrm{d}\mathbf{u}_a}{\mathrm{d}t} = \sum_b m_b \left(\frac{\boldsymbol{\sigma}_b}{\rho_b^2} + \frac{\boldsymbol{\sigma}_a}{\rho_a^2} + \Pi_{ab} \cdot \mathbf{I} \right) \nabla_a W_{ab} + \mathbf{g} \qquad [17]$$

$$\sigma_{a,ij} = -p_a \delta_{ij} + \tau_{a,ij} \qquad [18]$$

where $\boldsymbol{\sigma}$ is the total stress tensor.

To evaluate the shear stresses, the following SPH formulation for the velocity gradients will be adopted (Libersky *et al*., 1991):

$$\frac{\partial u_{a,i}}{\partial x_j} = \sum_b \frac{m_b}{\rho_b} \left(u_{b,i} - u_{a,i}\right) \frac{\partial W_{ab}}{\partial x_{a,j}} \qquad [19]$$

This method has been validated for materials with strength in PAM-CRASH by (Groenenboom 1997, 2002). The current model is similar to that used by (Ellero *et al*., 2002), with the visco-elastic model replaced by the Carreau model, but it differs from the implementation for incompressible flow by (Shao *et al*., 2003), who arrive at an expression for the viscosity similar to the usually adopted artificial viscosity.

To overcome numerical instabilities during the transient period when the flow is started, the artificial viscosity is linearly reduced and the Carreau model is linearly activated during a user-specified time interval.

Finally, the Murnaghan model (Equation 15) is also used as a constitutive equation. The parameters of this model are adjusted so that the compressibility of the fluid remains lower than few percents.

3.5. *Mixed FE-SPH*

Some advanced LCM modeling and simulations involve hydro-mechanical coupling when a foam core is compressed while manufacturing sandwich materials or when processes such as injection-compression or VARTM are used, for instance. In those cases, either flow induced deformations or forced deformations are present. Such interactions between resin and the moving structures (foam core, mold…) are modeled by one of the sliding interface algorithms available in PAM-CRASH. Sliding interfaces model the interaction between structures and parts of structures

that are not permanently connected by standard finite element connectivity conditions. The employed sliding interfaces is based on the well known penalty formulation, where geometrical interpenetrations between so-called slave nodes and contacting faces are penalized by counteracting forces that are in essence proportional to the penetration depth. The contact algorithm will automatically detect when a particle (slave) penetrates any segments (master) of the outer surface of the finite element of the foam. The contact thickness indicates the distance away from a contact face where physical contact is established. In this case the contact thickness should be representative of the particle size. The use of such interaction between the SPH and finite elements has been validated for a range of applications such as sloshing (Meywerk, 1999; Cha, 1999), heart valve opening (Haack, 2000) and impact of aeronautical structures on water (Pentecote, 2003).

4. Numerical schemes

4.1. *Explicit integration*

Temporal integration of Equations 13 and 14, is performed by a similar explicit method as for PAM-CRASH finite element nodes:

$$\frac{\left(\eta_a^{n+1}-\eta_a^{n}\right)}{\left(\Delta t\right)^{n+1/2}}=\sum_b m_b\left(\mathbf{u}_a^{n+1/2}-\mathbf{u}_b^{n+1/2}\right)\nabla_a W_{ab}^{n} \qquad [20]$$

$$\frac{\left(\mathbf{u}_a^{n+1/2}-\mathbf{u}_a^{n-1/2}\right)}{\left(\Delta t\right)^{n}}=-\phi_a\sum_b m_b\left(\frac{p_a^{n}}{\eta_a^{2}}+\frac{p_b^{n}}{\eta_b^{2}}+\Pi_{ab}^{n}\right)\nabla_a W_{ab}^{n}+\mathbf{g}-\phi_a^{2}\mu\,\mathbf{K}_a^{-1}\left(\frac{\tilde{\mathbf{u}}_a}{\eta_a^{n}}\right) \qquad [21]$$

$$\mathbf{r}_a^{n+1}=\mathbf{r}_a^{n}+\mathbf{u}_a^{n+1/2}\left(\Delta t\right)^{n+1/2} \qquad [22]$$

where the superscript denotes the time step, the tilde on $\mathbf{u}_a$ (Equation 21) the time step to be discussed below and $\mathbf{r}_a$ the particle coordinate vector. Note that all velocities are defined at intermediate (or half-integer) time steps whereas densities, pressure and positions are defined at integer time steps, rendering second-order accuracy. A numerically stable time step, accounting for finite elements, particles and any sliding interface, is determined automatically by the software during each solution step. Within the porous regions, the flow is usually dominated by the drag force contribution of Equation 21, which in equilibrium should be balanced by the pressure gradient, combined with gravity, if relevant. Hence, the drag term should be integrated in an implicit manner to guarantee numerical stability at an acceptable computational time step. Therefore $\tilde{\mathbf{u}}_a$ should be taken as $(\mathbf{u}_a)^{n+1/2}$. Since the expression for the drag force only depends on the properties of particle *a*, the unknowns at the new time step remain uncoupled from the neighboring particles.

Similarly, in the case of the Non-Newtonian formulation, Equations 16 and 17 will be integrated as:

$$\frac{\left(\rho_a^{n+1}-\rho_a^n\right)}{\left(\Delta t\right)^{n+1/2}}=\sum_b m_b\left(\mathbf{u}_a^{n+1/2}-\mathbf{u}_b^{n+1/2}\right)\nabla_a W_{ab}^n \qquad [23]$$

$$\frac{\left(\mathbf{u}_a^{n+1/2}-\mathbf{u}_a^{n-1/2}\right)}{\left(\Delta t\right)^n}=\sum_b m_b\left(\frac{\boldsymbol{\sigma}_a^n}{\rho_a^2}+\frac{\boldsymbol{\sigma}_b^n}{\rho_b^2}+\Pi_{ab}^n\cdot\mathbf{I}\right)\nabla_a W_{ab}^n+\mathbf{g} \qquad [24]$$

$$\mathbf{r}_a^{n+1}=\mathbf{r}_a^n+\mathbf{u}_a^{n+1/2}\left(\Delta t\right)^{n+1/2} \qquad [25]$$

where the total stress $\boldsymbol{\sigma}$ is the sum of the hydrostatic pressure and the viscous stress (Equation 18).

4.2. *Transition to the porous regions*

When a particle travels from a non-porous to a porous region, it will suddenly experience a high deceleration due to the drag force. To avoid the numerical instabilities that may arise from this situation, linear interpolation is used. The range corresponding to the representative smoothing length has been found to provide an adequate solution.

4.3. *Additional SPH features*

A well-known but undesirable feature of SPH is the tendency of the particle distribution of moving particles to become less homogeneous. A particle motion correction, introduced as XSPH by (Monaghan, 1994), but adapted to the apparent density η, is defined by:

$$\frac{\mathrm{d}\mathbf{r}_a}{\mathrm{d}t}=\mathbf{u}_a+\varepsilon\sum_b m_b\frac{\left(\mathbf{u}_b-\mathbf{u}_a\right)}{\frac{1}{2}\left(\eta_a+\eta_b\right)}W_{ab} \qquad [26]$$

The relative strength of this correction is given by ε which is usually taken close to 0.3. Other relevant features of the PAM-CRASH/SPH method are planes of symmetry, a variable smoothing length and non-interacting regions in space. The option of mirror particles (Morris, 1997) allows to introduce mathematically exact planes of symmetry. Non-interacting regions are also defined by parts of space in which particles do not experience mutual interaction. This option allows to define inflow regions of particles moving under the influence of inertia and external forces only. Those options have been used for the applications discussed below.

5. Examples of applications

5.1. *Isothermal isotropic filling*

Following is an example of mold filling simulation with isotropic permeability. A Newtonian fluid is injected in a complex 2D mold containing 50% of fiber reinforcement. The permeability of the fiber reinforcement is isotropic and constant in time ($K=10^{-10}$ m^2). The fluid viscosity is 0.001 Pa.s and the fluid inflow velocity is 0.05 $m.s^{-1}$ at both entries. Comparisons were made on flow front positions and pressure distributions with the well-established FE-based commercial simulation tool PAM-RTM (ESI, France) to model the RTM process including filling and curing. For this case, only the filling part based on Darcy's law, including flow front propagation has been used. Figure 2 shows the results of the simulations after 38 s (a and b) and 54 s (c and d) of injection. The comparison of the flow front positions using the SPH method (a and c) to the PAM-RTM ones (b and d) gives a good match. Minor differences in the filling sequence can be explained by the numerically enhanced compressibility used in the SPH simulations. Increasing the compressibility in SPH provides better agreement but at higher computational cost. In terms of injection pressure responses, the injection pressure obtained at the end of the injection is 0.07 MPa and 0.08 MPa from SPH and PAM-RTM simulations respectively. It is concluded that there is a quite reasonable agreement between the SPH method and PAM-RTM for isotropic porous media flow.

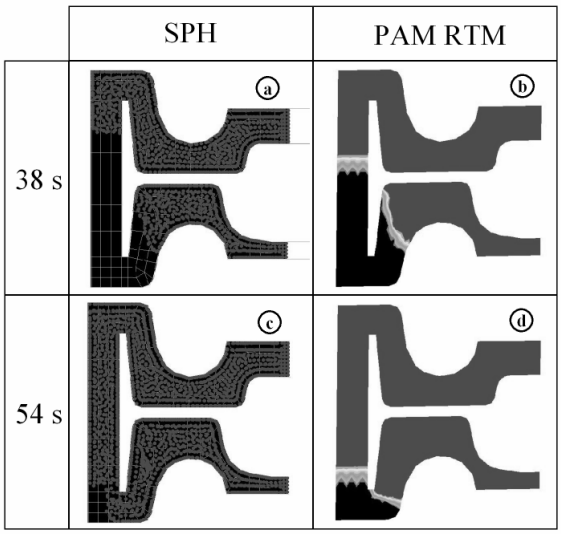

Figure 2. *Comparison of an isothermal isotropic RTM filling using the SPH method and PAM-RTM*

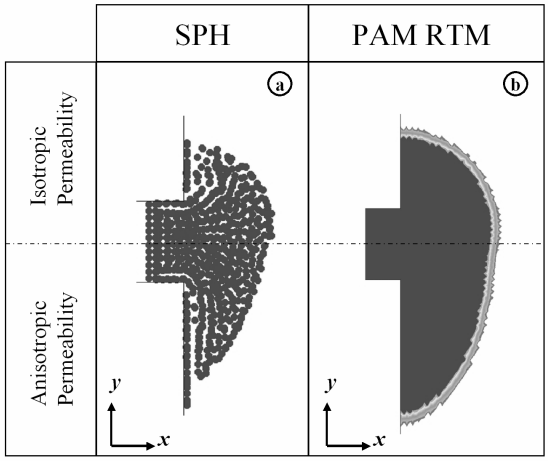

Figure 3. *Comparison of an isothermal anisotropic RTM filling using the SPH method and PAM-RTM*

5.2. *Isothermal anisotropic filling*

Orthotropic effects of the porous medium are easily incorporated in the method by considering the permeability **K**, to be a tensor. A Newtonian fluid is injected in a rectangular 2D mold containing 50% of fiber reinforcement. The permeability of the upper half of the mold is isotropic ($K=1.25\ 10^{-9}\ m^2$) while the bottom half is anisotropic ($K_{xx}=10^{-9}\ m^2$, $K_{xy}=K_{yx}=0.5\ 10^{-9}\ m^2$ and $K_{yy}=4.0\ 10^{-9}\ m^2$). Note that the off-diagonal terms (K_{xy} and K_{yx}) in the permeability tensor represent the angle between the simulation domain axes and the main flow directions of the fiber reinforcements. The simulation results shown in Fig. 3 demonstrate that the SPH method (a) is as accurate as PAM-RTM (b), and that the circular (upper half domain) and ellipsoidal (lower half domain) flow front profiles are respectively representative of an isotropic and anisotropic filling.

5.3. *Hydro-mechanical coupling*

RTM can be a very attractive single-step process for sandwich structures manufacturing. The two fiber-reinforced skins and the impermeable core are laid up in a mold cavity. Hydro-mechanical coupling is present when the pressure field developing while saturating the fiber-reinforced skins leads to shifting or compression of the core (Wirth *et al*, 1998; Binetruy *et al*., 2003). For such process, the skins are modeled as porous regions in which Lagrangian SPH particles are evolving. Figure 4 shows particles and finite elements modeling resin and sandwich core respectively.

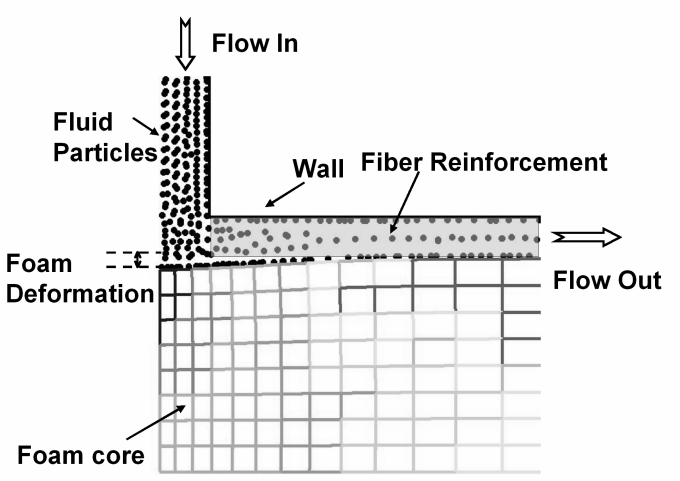

Figure 4. *Snapshot of the local foam deformation when hydro-mechanical coupling is present*

The injection is performed at constant flow rate. The equations for the deformation and stresses in the foam are solved by the explicit finite element algorithm. The choice has been made to employ the first-order, iso-parametric and under-integrated hexahedron elements with hourglass control of PAM-CRASH. Although specific material models for various types of foam are available within this software, a linear-elastic material behavior with initial internal compressive stress is assumed since the compression remains limited. When the foam is deformed because of resin pressure built-up, more volume becomes available to the resin. Both porosity and permeability increase leading to a discontinuity in the pressure response. User-defined subroutines have been developed to include porosity and permeability variations as a function of the local foam core displacement. This behavior simulated with the presented method agrees well with the physics and the experimental data. Full details, pressure and foam deformation results on hydro-mechanical coupling simulation using the mixed FE-SPH method are given in (Comas-Cardona *et al.*, 2005).

5.4. *Saturated permeability of fabrics*

In order to perform accurate LCM filling simulations, physical parameters such as fabric permeability are needed. It is well known that the experimental measurements of that fabric property is very delicate. Usually a fluid is injected at constant pressure (or constant flow rate) through several layers of fabric of cross section A and length L. Then pressure loss Δp and flow rate Q are measured, and the permeability K is calculated using Darcy's law:

$$K = \frac{QL\mu}{A\Delta p} \qquad [27]$$

The simulation of flow through a periodic cell should provide a reliable solution and avoid that experimental procedure. Numerically, an injection at constant flow rate could be performed. Then the pressure loss can be measured and the permeability is also given by Equation 27. However, another solution would be to start from a filled cavity, apply periodic boundary conditions and drive the fluid through the unit cell by gravity. For such flows, Darcy's law can be written as:

$$K_{xx} = \frac{\hat{u}_x \phi \mu}{\rho g} \qquad [28]$$

where $\hat{u}_x$ is the steady state average fluid velocity in the flow direction. A validation of this technique has been done for a Newtonian fluid flow through a rectangular pipe. Results of the validation for two viscosities are given in Table 1 using a 5 x 10 x 20 particle lattice. It can be seen that the theoretical permeability of a rectangular pipe (K_{th}) matches well the permeability obtained from the simulations (K_{SPH}). Calculations on a full size fabric cell (Figure 5) is currently under investigation.

Table 1. *Flow through a rectangular pipe (Re is the Reynolds number)*

	ρ (kg/m$^{3)}$	μ (Pa.s)	g (m/s^2)	K_{SPH} (m^2)	K_{th} (m^2)	$Re = \frac{\rho \hat{u} h}{\mu}$
Sim 1	1	1	1	$5.5\ 10^{-2}$	$5.7\ 10^{-2}$	$5.5\ 10^{-2}$
Sim 2	1	10	1	$5.4\ 10^{-2}$	$5.7\ 10^{-2}$	$5.4\ 10^{-3}$

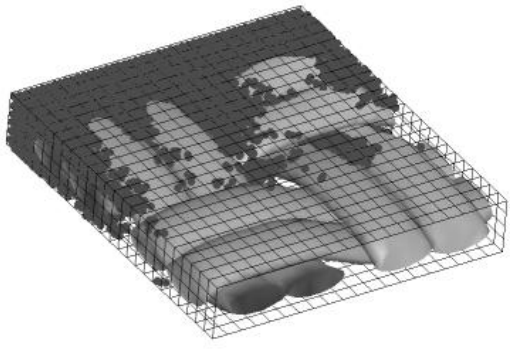

Figure 5. *Snapshot of the filling of a periodic fabric unit cell*

6. Discussion and conclusions

This paper presents the mathematics and numerical schemes for a unified approach to LCM processes at various scales of discretization, using a mixed FE-SPH approach. It has been demonstrated that the SPH method allows to simulate mold filling in both isotropic and anisotropic porous media, and viscous flow to determine permeability. In combination with Finite Elements, hydro-mechanical coupling during an RTM process may be simulated as well.

Flow front and pressure levels obtained with the FE-SPH method may slightly differ from experiments because of the limited compressibility allowed in the solution (Equation 15). Therefore a compromise need to be found between reducing compressibility and obtaining results at a reasonable CPU. The level of these differences is, however, surpassed by the variations in the results due to the inaccuracies in the measured physical input parameters. For regular filling, these inaccuracies propagate in a linear manner, but with hydro-mechanical coupling, the variations in the results may become much bigger.

The generic FE-SPH method is not expected to prevail for regular resin filling simulations since FDM or FEM filling tools are faster to use. However, when coupling is of interest, the SPH-FE method does provide an attractive alternative. A major advantage of this method with respect to PAM-RTM and similar software is that it allows the interactive coupling with the structural deformation leading to a completely different flow because of permeability variations and the formation of channels (preferential flow) in between the fiber reinforcement and the foam for instance. Therefore, the potential of the method relies on its Lagrangian formulation as well as its ability to interact with finite elements. Also, it would be of interest for mesoscopic and microscopic flows in unit fabric cells. More work could involve the hydro-mechanical coupling between the flow and the fibers, and the permeability measurement for sheared fabrics for instance.

Future developments for a more powerful LCM simulation tool would be to incorporate the equation of energy to solve for non-isothermal processes. This original method provides a suitable solution for various coupled phenomena since the integration of many physical effects is rather straightforward in the SPH formulation and implementation. This feature is an important asset of the method

Acknowledgements

The authors would like to thank S.V. Lomov and I. Verpoest (KUL, Belgium) for providing the fabric unit cell.

7. References

Achilleos E., Georgiou G., Hatzikiriakos S., “On numerical simulations of polymer extrusion instabilities”, *Appl. Rheol*., Vol. 12, 2002, pp. 88-104.

Acheson J.A., Simacek P., Advani S.G., "The implications of fiber compaction and saturation on fully coupled VARTM simulation", *Comp. Part A*, 2004, Vol. 35, pp. 159-169.

Belov E.B., Lomov S.V., Verpoest I., Peters T., Roose D., Parnas R.S., Hoes K., Sol H., "Modelling of permeability of textile reinforcements: lattice Boltzmann method", *Comp. Sci. Tech.*, Vol. 64, No. 7-8, 2004, pp. 1069-1080.

Binetruy C., Advani S.G., "Foam core deformation during liquid molding of sandwich: Modelling and experimental analysis", *J. Sand. Struc. Mat.*, Vol. 5, No. 4, 2003, pp. 351-376.

Cha H., Lee I., Choi H.Y., "Industrial applications of PAM-SHOCK using SPH", In: *PAM Users Conference in Korea HANPAM '99*, Seoul, November 15-16, 1999, pp. 253-265.

Comas-Cardona S., Groenenboom P.H.L., Binetruy C., Krawczak P., "A generic mixed FE-SPH method to address hydro-mechanical coupling in liquid composite moulding processes", *Comp. Part A*, 2005, To be published.

Ellero M., Kroeger M., Hess S., "Viscoelastic flows studied by Smoothed Particle Dynamic", *J. Non-Newtonian Fluid Mech.*, Vol. 105, 2002, pp. 35-51.

Farina A., Cocito P., Boretto G., "Flow in deformable porous media: Modelling and simulations of compression moulding processes", *Mathl. Comput. Modelling*, Vol. 26, No. 11, 1997, pp. 1-15.

Gingold R.A., Monaghan J.J., "Smoothed particle hydrodynamics: Theory and application to non-spherical stars", *Mon. Not. R. Astr. Soc.*, Vol. 181, 1977, pp. 375-389.

Groenenboom P.H.L., Copper cylinder impact at high velocity: Numerical Simulation using SPH and Finite Elements in PAM-SHOCK, ESI internal report, 2002.

Groenenboom P.H.L., "Numerical simulation of 2D and 3D hypervelocity impact using the SPH option in PAM-SHOCK", *Int. J. Impact Eng.*, Vol. 120, 1997, pp. 309-323.

Haack C., On the use of a Particle Method for Analyis of Fluid-structure Interaction, Sulzer Innotech Report STR TB2000 014, June, 2000.

Han K., Lee L.J., Liou M., "Fibre mat deformation in liquid composite molding, II: Modelling", *Polym. Comp.*, Vol. 14, No. 2, 1993, pp. 151-160.

Kang M.K., Lee W.I.; Hahn H.T., "Analysis of vacuum bag resin transfer molding process", *Comp. Part A*, Vol. 32, 2001, pp. 1553-1560.

Libersky L.D., Petschek A.G., Smooth Particle Hydrodynamics with strength of materials, In: Trease H.E., Fritts M.J. and Crowley W.P. (Ed.), Advances in Free-Lagrange Methods, June 1990, Lecture Notes in Physics, Vol. 395, Spinger, New York, 1991, pp. 248.

Lucy L.B., "A Numerical Approach to the Testing of Fusion Process", *Astron. J.*, Vol. 88, 1977, pp. 1013-1024.

McCabe C., Manke C.W., Cummings P.T., "Predicting the Newtonian viscosity of complex fluids from high strain rate molecular simulations", *J. Chem. Phys.*, Vol. 116, No. 8, 2002, pp. 3339-3342.

Meywerk M., Decker F., Cordes J., "Fluid-structure interaction in crash simulation", *Proc. Inst. Mech. Engrs*., Vol. 214, 1999, pp. 669-673.

Monaghan J.J., "Simulating free surface flows with SPH", *J. Comput. Phys*., Vol. 110, 1994, pp. 399-406.

Monaghan J.J., Gingold R.A., "Shock Simulation by the Particle Method SPH", *J. Comput. Phys*., Vol. 52, 1983, pp. 374-389.

Morris J.P., Fox P.J., Zhu Y., "Modelling low Reynolds number incompressible flows using SPH", *J. Comput. Phys*., Vol. 136, 1997, pp. 214-226.

PAM-CRASH Notes Manual, ESI-Group Trademark, 2001.

Pentecote N., Kohlgrueber D., Kamoulakos A., "Simulation of water impact problems using the Smoothed Particle Hydrodynamics Method", *ICD'03 conference*, Lille, France, December, 2003.

Pillai K.M., "Governing equations for unsaturated flow through woven fibre mats, Part 1. Isothermal flows", *Comp. Part A*, Vol. 33, No. 7, 2002, pp. 1007-1019.

Sawley M., Cleary P., Ha J., "Modelling of Flow in Porous Media and Resin Transfer Moulding using Smoothed Particle Hydrodynamics", *2nd Int'l Conference on CFD in Minerals and Process Industries*, CSIRO, Melbourne, Australia, 6-8 Dec, 1999, pp. 473-478.

Shao S., Lo E.Y.M., "Incompressible SPH method for simulating Newtonian and non-Newtonian flows with a free surface", *Adv Water Resources*, Vol. 26, No. 7, 2003, pp. 787-800.

Trochu F., Gauvin R., Gao D.M., "Numerical analysis of the Resin Transfer Molding process by the Finite Element Method", *Adv. Polym. Tech*., Vol. 12, No. 4, 1993, pp. 329-342.

Tucker III C.L., Dessenberger B., "Governing equations for flow and heat transfer in stationary fibre beds", Advani SG ed., Flow and *Rheology in Polymer Composite Manufacturing*, Amsterdam, Elsevier, 1994, p. 257-323.

Wirth S., Gauvin R., "Experimental analysis of core crushing and core movement in RTM and SRIM foam cored composite parts", *J. Reinf. Plast. Comp*., Vol. 17, No. 11, 1998, pp. 964-988.